

Imprinting Bone Surface Topography on Cast Metal

Aybüke Üretmen^{a*}, Caner Demir^b, Vram Odabaşoğlu^c, Abdulhalim Kılıç^a

^aDepartment of Molecular Biology and Genetics, Istanbul Technical University, Istanbul, Türkiye

^bResearch and Development Department, Tayf Biotechnology, Istanbul, Türkiye

^cTeknik Döküm Coating Materials Inc., Istanbul, Türkiye

*Corresponding author's email: uretmen20@itu.edu.tr

Abstract

Chemical and physical features including stiffness and roughness texture of the biomaterials are important factors for in-vitro and in-vivo cell behaviour. Bone mimetic topography of the biomaterials can enhance the cell adhesion, cell proliferation and differentiation, leading to promoted bone tissue regeneration. In this study, a new technique for transferring the topography of the decellularized cortical bone to the cast metal was described. Imprinting efficiency and accuracy were high, as shown with light microscopy and atomic force microscopy. This method will pave the way for the development of new materials for bone tissue engineering.

Keywords

Bone topography, Biomimetic, Topography Imprinting, Moulding, Metal Casting

1. Introduction

In human body, cells proliferate and differentiate in various natural scaffold environments such as hard bones and soft tissues. Different tissues have different physical and chemical properties which determine the behaviour of the cells along with protein interactions. Therefore, biomaterials which are implanted into the body need to carry properties suitable for the tissue type for better biocompatibility. Cell differentiation and proliferation are affected by the physical nature of the external surfaces on which cells are attached. [1, 2] These include stiffness, electrical charge distribution, roughness and topography of the surface. [3, 4] Cell adhesion to surfaces and 3-dimensional positioning according to surface topography rearrange the intracellular matrix of the cell. These rearrangements trigger changes in organelle distribution, protein reorganizations and protein interactions also gene expressions in the cells. [5, 6, 7, 8] Cell movement and migration on a surface with varying roughness distribution cause dynamic changes in cell structure limited by the said surface properties of the materials. [9, 10] These are important aspects in developing biomaterials.

Biomaterials can be developed for different applications and purposes including in-vitro cell or tissue development, in-vivo permanent or transient implants and in-vivo degradable

implants. Except transient use of the biomaterials, most of the biomaterials need better cell adhesion and compatible cell-material surface interaction. Recent studies investigate the topographic effects of biomaterials on cell growth, cell orientation and cell differentiation. [11] Based on these knowledge, different physical, chemical or biologic methods are being developed and used to form the material surfaces. These can include chemical etching, high voltage plasma treatment, laser ablation, physical abrasion, biological modifications and polymer imprinting [12, 13, 14, 15, 16].

For bone tissue which is more stiff than other body tissues, both surface topography and material hardness level is important in bone tissue engineering and bone implant development. Imprinting bone surface to different polymers such as PDMS (polydimethylsiloxane) is possible, but they lack the necessary hardness values. This limits the development of harder materials resembling bone. It is a great advantage to develop hard metals with bone structure imprinted on. Hard metal surfaces can be used directly or used as master moulds for developing different types of surfaces. Also, hard metals can be used as master moulds for long term usage and can provide repeatability in the bone mimicking surfaces. For these purposes, we developed a method that can be used to mimic the bone surface on metal. In this paper, a

new method for transferring bone surface topography to cast metal surfaces is explained.

2. Materials and Methods

2.1. Materials

2.1.1. Preparing decellularized bone

Thigh bone of male calf, aged 12 months and slaughtered within 24 hours, was used. Phosphate buffer saline (PBS) was prepared from sodium chloride (Merck, EMSURE), potassium chloride (Merck, EMSURE), potassium dihydrogen phosphate (Merck, EMSURE), di-sodium hydrogen phosphate dihydrate (Merck, EMSURE) for washing steps. Sodium dodecyl sulfate (Merck, Ph. Eur) and ethanol (Merck, Absolute) were used for disrupting cells and dissolving organic cell components. di-Sodium tetraborate (Borax) (%98<) used for cross-linking bone structure. Penicillin/streptomycin (Euroclone) and gentamicin were used as antimicrobial agents.

2.1.2. Imprinting bone surface topography on metal

Silicone jewellery moulding rubber (Castaldo, No shrink pink) was used for imprinting bone topography to create a reusable mould. Mould rubber vulcanizer (Teknik Döküm, VPP12-20) was used to vulcanize rubber. A metal rod and scalpel were used to create wax injection channels in the rubber moulds. Wax (Freeman flakes wax, aqua green) was used to fill the bone cavity in the rubber mold. To melt wax and fill in the rubber mold, wax injection device (Teknik Döküm, MK-2000) was used. An air compressor with adjustable air valve was used to adjust pressure during wax injection. Plaster (Chang Jewellery Powder Co., Ltd. EagleTm) was used to surround wax tree tightly and to form cavities for metal. Mechanical stirrer (Mtops, MS3020) was used to mix plaster and water properly. Vacuum chamber providing vibration (Teknik Döküm VH-1) was used in the plaster casting step. The furnace (Teknik Döküm, DF-422D) was used for melting wax in the plaster and to crystallize the plaster. Brass alloy (Pandora Alloys s.r.l, BR88/12-S, %88 Copper, Zn) was used as a metal to transfer bone topography on it. Vacuum casting device (Teknik Döküm, VD-25V) and electric melting furnace (Vevor, GF1100ND3) were used for casting metal.

2.1.3. Surface topography characterization

Compression test was conducted in CheckWay WDW 20KN. Stereo microscope (SOIF) was used for investigating the bone surface transfer to the wax and brass surface. AFM (Atomic force microscopy) was conducted on bone surfaces and cast metal surfaces. AFM analysis were conducted with Nanomagnetism Instruments model ezAFM. For image processing, GIMP and ImageJ used.

2.2. Methods

2.2.1. Preparing decellularized bone

External surfaces of the bones (cortical) were used for topographic transfer purpose. Bones had a periosteum layer

which needed to be removed first by cutting with scalpel and taken out by tissue forceps. Then, thigh bone was cut into blocks with surface sizes approximately 5 mm x 10 mm. Thickness can vary according to the different bone locations, ranging from 8 mm to 13 mm. A tabletop bandsaw was used in the cutting process. After cutting, bone blocks were immersed into PBS, containing %1 penicillin/streptomycin and %1 and gentamicin and waited for 10 minutes. Bones were placed into 50 ml conical centrifuge tubes containing 80-90 °C deionized water and rolled for 1 minute in high speed and water was discharged. Fresh hot water is filled into the tube and process repeated for 5 times. After this stage, bone blocks can be frozen for long term storage in -20 °C freezer. Bone can lose its surface hardness in the decellularization process, which can lead to topographic memory loss in the imprinting processes. To overcome this problem, we have developed a crosslinking method to keep bone surface hardness. For crosslinking bone to preserve its structural integrity, %1 (w/v) borax solution is prepared in deionized water which was preheated to 39-40 °C. Bones were placed in the solution and heated to 80 °C slowly to prevent temperature shock, and kept at that temperature for 4 hours. On-off vacuum cycles were applied for better penetration of the solution into the bone structure and for more effective cleaning of the complex bone structures. In this process, vacuum at 0.1 bar was applied instantaneously using a manual valve, from a vacuum chamber into the vacuum oven. This was repeated with 15 minutes intervals. Between steps, vacuum is kept at 0.4 bar to keep water boiling in low pressure.

After heating process, solution was removed by filtration and bones were rinsed with deionized water. Bones were placed into tubes containing deionized water and vortexed at high speed for 1 minute. Water is discharged and bones were immersed into fresh deionized water preheated to 40 °C and incubated for 1 hour on the shaker. Water is removed by filtration, and bones were dried on the filtration paper to remove excess water. After these steps, ethanol and SDS solutions were applied to bone blocks to remove cell debris. Bones were immersed into %75 ethanol solution and vortexed for 2 minutes, excess solution is filtered out. Bones were placed into %2.5 SDS solution and incubated for 8 hours at 40 °C with continuous shaking. After solution is discharged, bones were vortexed in %25 ethanol for 1 minute and incubated in %25 ethanol at 40 °C for 1 hour while shaking. Vortexing and incubating set was conducted for two times. After filtering out the liquid, the same process was conducted for two times using %75 ethanol solution. Bones were filtered and immersed in absolute ethanol and the process repeated for two times again. To remove ethanol, bones were placed into water and vortexed for 1 minute and incubated in fresh water at 40 °C for 2 hours. Water was changed at 30 minutes intervals. Bone blocks were immersed in PBS solution,

vortexed for 1 minute and incubated for 30 minutes at 40 °C by shaking and vortexed again for 1 minute in fresh PBS. Bones were dried at 40 °C for 2 hours.

2.2.2. Imprinting bone surface topography on metal

To transfer bone surface structure to metal, various steps are necessary.

Transferring bone surface topography to silicone rubber

Bone was used as positive surface pattern and silicon jewellery rubber was used as the first transfer medium for surface topography of the bone. Silicon moulding rubbers were cut and placed in the preheated (200 °C) rectangular aluminium mould. The bone blocks were placed horizontally on the silicone rubber. Additional layers of silicone rubber were placed on the bone blocks, then the other preheated aluminium mould lid was placed to cover all the rubber layers. This structure was placed into the mould rubber vulcanizer, which was preheated to 155 °C. In order to activate crosslinking of the rubber, the rubber was vulcanized at 155 °C for 38 minutes under 6 bar air pressure. After vulcanization, the aluminium mould containing rubber was cooled for 30 minutes in room temperature and the rubber mould was cut in half in the horizontal plane. Bone pieces were removed from the rubber mould carefully. The channels on the silicone rubber mould were carved using a heated metal rod and a scalpel for wax injection.

Transferring surface topography from silicone rubber to wax

The prepared silicone rubber mould was used as an intermediate mould to transfer the bone surface topography to the wax. The injection wax was melted in the pot of the wax injection device at 80 °C. The injection device was connected to the air compressor to supply air pressure (0.6 bar) to the melted wax. The silicone rubber mould, with the negative pattern of the bone surface topography inside, was pressed against the wax injection nozzle on the device while firmly pressing with metal plates from each side. The melted wax was filled into the cavities through the channels opened in the silicone rubber mould and hardened after approximately 2 minutes. The bone surface topography was transferred to the wax surface. These formed wax moulds were removed from the silicone rubber mould without damaging their surfaces.

Transferring surface topography from wax to plaster

A wax rod was prepared by pouring wax into a thin hollow cylinder and after cooling the wax rod was placed in the middle of a lid. Using a soldering iron at 100 °C, bone topography imprinted wax moulds were stuck to the wax rod with an acute angle upward to create a wax tree. Upward connection is important for having mostly laminar flow in the metal casting steps to prevent surface distortions. A metal hollow cylinder containing vacuum holes was placed around the wax tree and sealed by the lid from downside. The holes on the cylinder were sealed with a tape before the plaster was cast to prevent

leakage. The cylinder containing tree was placed inside the vacuum vibration chamber.

To prepare plaster, 1220 millilitres of water was measured, 3050 grams of plaster powder was weighted and placed on the water for the cylinder with diameter 120 mm and height 200 mm. The water/powder ratio is important for the final strength of the plaster and its porosity ratio, which is important for metal casting process. Water and plaster powder were mixed first with a glass rod and then with a mechanical stirrer for 4 minutes. Vacuum was applied to the plaster mixture for 1 minute to remove air bubbles. After this step, the cylinder flask which was in the vacuum chamber was filled with plaster solution. Vacuum and vibration were immediately applied to the chamber for 2 minutes. The plaster was dried at room temperature for 2 hours and the tape around the flask was removed.

Transferring surface topography from plaster to metal

The dried plaster was placed in the furnace. The furnace temperature was gradually increased to 200 °C in 1 hour. The temperature was kept at 200 °C for 2 hours to completely melt the wax and let the wax flow down from the plaster cavities. After 2 hours, the furnace temperature was gradually increased to 730 °C in 3 hours and maintained at that temperature for 4 hours. Then, the furnace temperature was gradually reduced to 400 °C before the metal casting step. When the plaster temperature reached to 400 °C, the cylinder flask was placed in the vacuum casting device. Vacuum was applied before casting metal and during the casting process to prevent air sockets and to allow efficient metal-plaster surface interaction.

The brass alloy was melted in a graphite melting pot at 1110 °C in the electric melting furnace. The molten alloy was then immediately cast into the plaster and argon gas was applied immediately. When metal colour becomes red, the cylinder flask was taken from the casting device and was kept in the water for cooling. Then, with a hammer and pressurized water (10 bar), the plaster was broken. The metal tree which has the bone surface topography with positive pattern were removed from plaster.

2.2.3. Surface topography characterization

Compression test was applied with a 1 mm/min rate to 15 mm x 20 mm bone sections. Epoxy resin was applied into the remaining trabecular bone under the cortical bone to prevent crushing. Stereo microscopy was used for investigating the efficiency of bone surface transfer to the wax and brass surfaces. Microscopy photos were processed in ImageJ and GIMP for distinguishing structures better. AFM was conducted on the bone block and cast metal surfaces. For both bone blocks and cast metal, a 40 µm x 40 µm area was examined with a speed of 4 µm/sec. The imaging was conducted in non-contact mode. Gwyddion 2.57-1 software was used to analyse and inspect AFM raw data.

2.3. Results and Discussion

A schematic summary of the developed method for transferring bone surface structures to cast metal can be seen in Figure 1. In the first step involving silicon rubber vulcanization, sufficient pressure must be applied to the mold. Otherwise, it was observed that bone structure was not transferred efficiently to rubber. Also, the type of silicon rubber is important, which affects imprinting details of topographic changes. On the other hand, bone have some structures on its surface which have layered properties and having some sharp-edged. Silicon rubber infiltrates into these areas and fill these volumes and when mold was released from bone some micro particles of the bone surface can be trapped in these areas or rubber can be torn in microscale. To overcome this problem, having a silicon rubber with sufficient stiffness which is in the range 38-45 shore hardness value is necessary. Shrinkage of the silicon mold can increase this problem and can also lead to deformed topography transfer. For this purpose, it was found that no-shrink rubber type was a better choice.

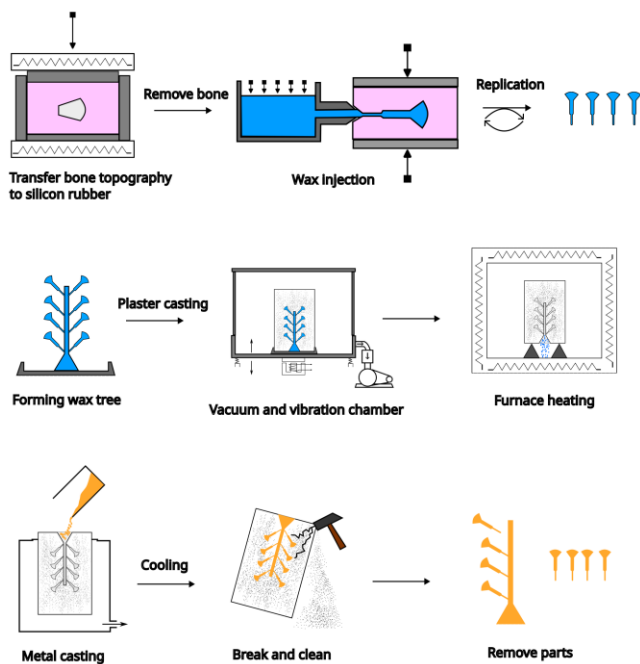


Figure 1. Summary of the process for transferring bone surface topography to metal.

The quality and hardness of the bone after the decellularization process can have an effect on the surface quality of the silicone rubber. Any method involving ultrasonication or other harsh treatment can lead to produce a more brittle and softer surface. This can cause some loss of the topographical properties of the bone from its original state, especially when transferring the bone surface to other surfaces, and can cause micro-particles entrapped in the silicone mould surface. We have developed on-off and continuous vacuum treatment cycles in the decellularization process for more efficient cleaning instead of this method to preserve surface structure. Borax application

has been found to preserve the strength of the cortical bone, having 13.3 GPa for natural dry bone and 11.7 GPa for decellularized dry bone, but more importantly, it is the surface hardness of the bone. More analysis must be conducted to measure the surface stiffness with a roughness meter. To explain the effect of borax in terms of chemical reactions, it must be considered that collagen molecules contain functional groups that can react with di-sodium tetraborate (borax). The borate ions in borax can react with the hydroxyl and amino groups present in collagen molecules, resulting in the formation of covalent bonds between the collagen molecules. When borax comes into contact with collagen molecules, it reacts with hydroxyl groups (-OH) present in the amino acid residues of collagen. Specifically, the hydroxyl groups are present on the side chains of three amino acids - proline, hydroxyproline, and lysine - which are commonly found in collagen. Borax reaction with amino acids forms stable covalent linkages between collagen molecules, resulting in crosslinking. Crosslinking of collagen molecules can enhance their stability under high temperature and solvent applications.

After bones were taken out from silicon rubber, any remaining were cleaned with brush and dry air flow. This ensured cleaner surface before wax injection. Using a wax that won't form ash in the heating step of the plaster is important, as ash remaining can decrease cast metal and plaster surface interactions. Silicon rubber containing moulded wax was shown in the figure 2. After forming the tree with these wax moulds and placing the tree into the cylinder filled with plaster afterward, the wax moulds are ready for surface transfer to plaster. The water/powder ratio is important for the final strength of the plaster and its porosity ratio, which is important for metal casting process. Controlled slow temperature increase was applied in the process, as heating is important for having the proper porosity of the plaster without having large hollow areas and cracks. After hardening of the plaster, it is ready for metal casting (Figure 3).

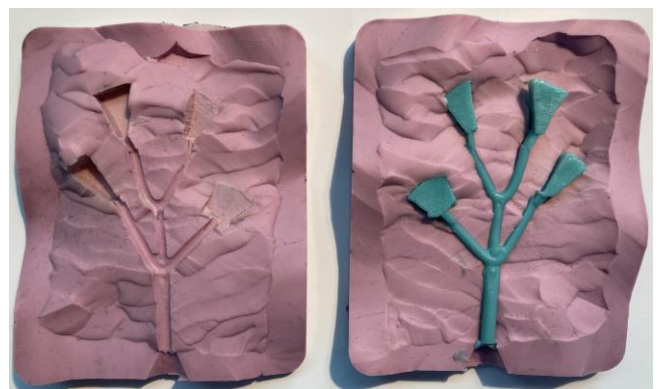


Figure 2. Moulded silicone rubber after filled with wax.



Figure 3. Plaster in the cylinder with holes after hardening and tape removed.

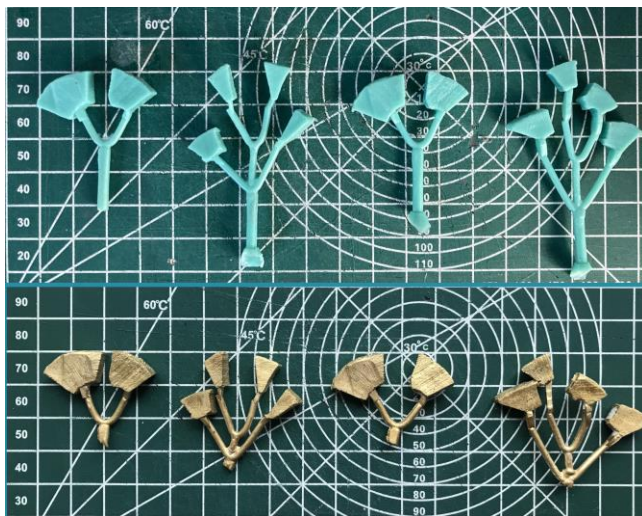


Figure 4. Upper photo with wax moulds before metal casting and lower photo with brass moulds after casting.

In the metal casting process, we have chosen brass for its properties against corrosion and tear, also for its mechanical strength and ease of casting. Before metal casting, the plaster should be in a suitable temperature range to prevent rapid cooling of the metal in the plaster. This ensures the successful transfer of a more detailed surface structure from the plaster to the metal. Plaster temperature is affected by the dimensions of the cylinder, so there is not a fixed temperature for a certain metal. Vacuum application is important in the casting step to ensure complete transfer of plaster surface to metal. Wax moulds before casting and brass moulds after casting were shown in the Figure 4.

Microscopy images show surface structures of natural bone, intermediate wax surface and bone mimicking metal surfaces (Figure 5). There are different macro and microstructures on the natural bone surfaces, which were observed to be transferred onto cast metal. Grooves and peaks were clearly seen in the bone and cast metal surface. It is important to note that though rubber, wax, and plaster were used as intermediate topography transfer mediums, the process had a high efficiency for transferring surface structures. Closer inspection

shows characteristic surface properties of certain bone areas transferred to the metal, including sharper edges (Figure 6).

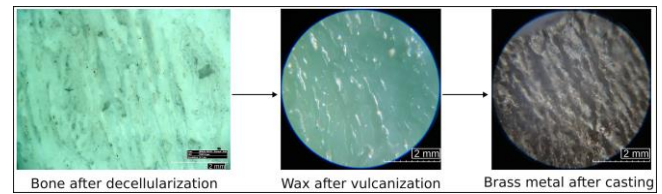


Figure 5. Macro structures on bone, intermediate wax and bone mimetic casted metal. (Scale bar is 2 mm)

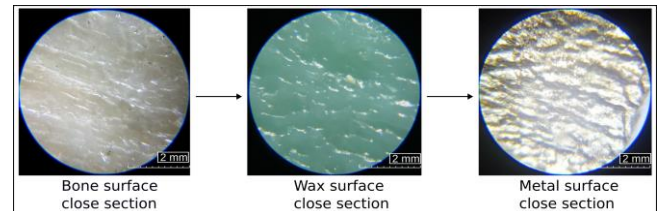


Figure 6. Micro structures on bone, intermediate wax and bone mimetic casted metal. (Scale bar is 2 mm)

There are different surface characteristics which were successfully transferred onto metal surface. As bone surface has a heterogeneous structure in 3-dimensional space, irregular surface topography distribution is expected on metal surface. This distribution can be observed on different areas of the cast metal (Figure 7). A metal stick with a length of 1 mm and thickness of 0.1 mm was placed on the imprinted metal to show macro and micro surface pattern.

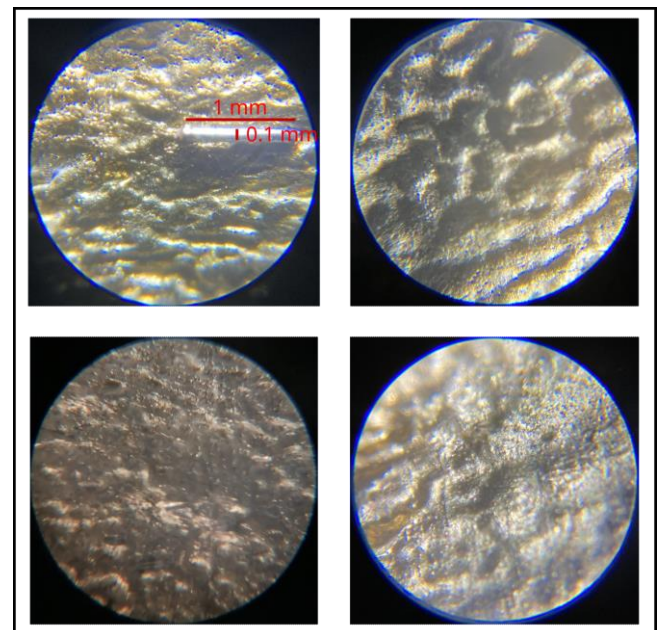


Figure 7. Heterogenous surface topography distribution shown in different areas of casted metal surface. (Scale bar is 1 mm)

AFM analysis has shown that microstructures such as ridges, cavities, and slopes were transferred to the metal surface with a high efficiency (Figure 8). We have examined shallow areas for comparison of bone and metal surfaces to observe microscale transfer efficiency. Roughness average values for

bone and cast metal were 1.382 μm and 1.411 μm , respectively. Root-mean-square roughness values for bone and cast metal were 442.3 nm and 353.9 nm, respectively. Maximum peak height values for bone and cast metal were 1.662 μm and 1.787 μm , respectively. These data show that our process is sensitive and has a high accuracy in terms of topography transfer of bone onto cast metal.

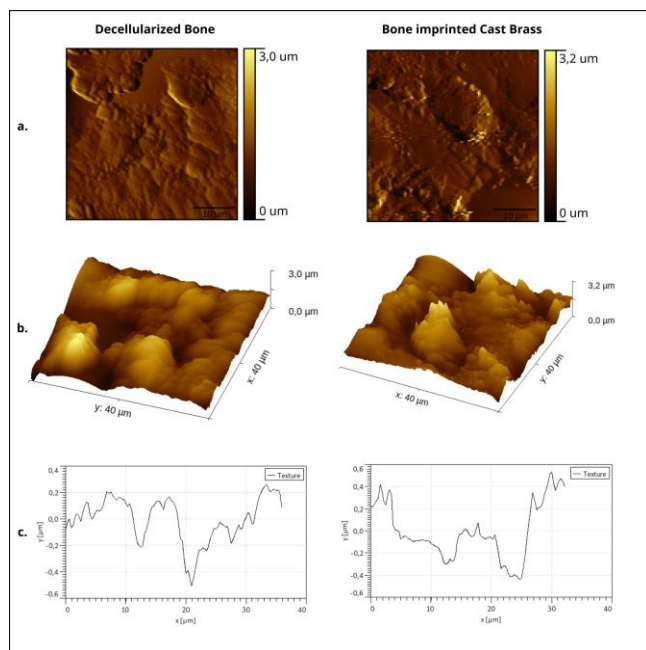


Figure 8. Left column side contains pictures and graph for decellularized bone and right side for cast brass metal. a. 2D AFM images (10 μm scale bar). b. 3D AFM images. c. Roughness texture in random line.

3. Conclusion

A new method for transferring bone topography to hard metal surfaces has been described. This method expands the possibilities for developing new types of bone biomaterials. The method ensures a highly efficient transfer of the bone surface to the cast metal, generally without loss of macro and microstructures. The metal cast bone-mimicking surfaces can be used as moulds for other materials, such as resins, biodegradable polymers, and ceramics. Additionally, metals have high compressive strength, so polymers can be heat pressed onto metal moulds without using solvents, which are typically incompatible for in-vivo applications. Special resins and composite materials can be formed using metal bone moulds for use in in-vitro or in-vivo tissue engineering applications.

For future studies, it is possible to cast high-melting-point metals, such as titanium, with bone-mimicking surfaces that can be used in certain in-vivo implants.

Authors' Contributions

Conceptualization: Aybüke Üretmen, Caner Demir; methodology: Aybüke Üretmen, Vram Odabaşoğlu, Caner

Demir; supervision: Aybüke Üretmen; writing: Aybüke Üretmen; review and editing: Abdulhalim Kılıç; resources: Aybüke Üretmen, Caner Demir, Vram Odabaşoğlu; materials: Aybüke Üretmen, Caner Demir; data collection: Aybüke Üretmen; literature review: Aybüke Üretmen.

Declaration of Competing Interest

The authors declare that they have no known competing financial interests or personal relationships that could have appeared to influence the work reported in this paper.

Acknowledgement

We thank the company of Teknik Döküm for providing technical instruments and for their technical support.

References

- [1] Haihong Liao, Ann-Sofie Andersson, Duncan Sutherland, Sarunas Petronis, Bengt Kasemo, Peter Thomsen, Response of rat osteoblast-like cells to microstructured model surfaces in vitro, *Biomaterials*, Volume 24, Issue 4, 2003, Pages 649-654, ISSN 0142-9612, [https://doi.org/10.1016/S0142-9612\(02\)00379-4](https://doi.org/10.1016/S0142-9612(02)00379-4).
- [2] Biggs MJ, Richards RG, Gadegaard N, Wilkinson CD, Dalby MJ. The effects of nanoscale pits on primary human osteoblast adhesion formation and cellular spreading. *J Mater Sci Mater Med.* 2007 Feb;18(2):399-404. doi: 10.1007/s10856-006-0705-6. PMID: 17323174.
- [3] Altankov, G., Richau, K. and Groth, T. (2003), The role of surface zeta potential and substratum chemistry for regulation of dermal fibroblasts interaction. *Mat.-wiss. u. Werkstofftech.*, 34: 1120-1128. <https://doi.org/10.1002/mawe.200300699>.
- [4] Han SB, Kim JK, Lee G, Kim DH. Mechanical Properties of Materials for Stem Cell Differentiation. *Adv Biosyst.* 2020 Nov;4(11):e2000247. doi: 10.1002/adbi.202000247. Epub 2020 Oct 9. PMID: 33035411.
- [5] Qian Sun, Qiang Wei, Changsheng Zhao, How do the cells sense and respond to the microenvironment mechanics? *Chinese Science Bulletin*, Volume 66, Issue 18, 2021, Pages 2303-2311, ISSN 0023-074X, <https://doi.org/10.1360/TB-2020-1069>.
- [6] Wolfenson H, Yang B, Sheetz MP. Steps in Mechanotransduction Pathways that Control Cell Morphology. *Annu Rev Physiol.* 2019 Feb 10;81:585-605. doi: 10.1146/annurev-physiol-021317-121245. Epub 2018 Nov 7. PMID: 30403543; PMCID: PMC7476682.
- [7] Alberto Elosegui-Artola, Xavier Trepate, Pere Roca-Cusachs, Control of Mechanotransduction by Molecular Clutch Dynamics, *Trends in Cell Biology*, Volume 28, Issue 5, 2018, Pages 356-367, ISSN 0962-8924, <https://doi.org/10.1016/j.tcb.2018.01.008>.
- [8] Fletcher, D., Mullins, R. Cell mechanics and the cytoskeleton. *Nature* 463, 485–492 (2010). <https://doi.org/10.1038/nature08908>.
- [9] Wong PC, Song SM, Tsai PH, Nien YY, Jang JS, Cheng CK, Chen CH. Relationship between the Surface Roughness of Biodegradable Mg-Based Bulk Metallic Glass and the Osteogenic Ability of MG63 Osteoblast-Like Cells. *Materials (Basel).* 2020 Mar 6;13(5):1188. doi: 10.3390/ma13051188. PMID: 32155846; PMCID: PMC7085092.
- [10] Lange R, Lüthen F, Beck U, Rychly J, Baumann A, Nebe B. Cell-extracellular matrix interaction and physico-chemical characteristics of titanium surfaces depend on the roughness of the material. *Biomol Eng.* 2002 Aug;19(2-6):255-61. doi: 10.1016/s1389-0344(02)00047-3. PMID: 12202192.
- [11] Qian Sun, Yong Hou, Zhiqin Chu, Qiang Wei, Soft overcomes the hard: Flexible materials adapt to cell adhesion to promote cell mechanotransduction,

Bioactive Materials, Volume 10, 2022, Pages 397-404, ISSN 2452-199X, <https://doi.org/10.1016/j.bioactmat.2021.08.026>.

[12] Sjöström T, Dalby MJ, Hart A, Tare R, Oreffo RO, Su B. Fabrication of pillar-like titania nanostructures on titanium and their interactions with human skeletal stem cells. *Acta Biomater.* 2009 Jun;5(5):1433-41. doi: 10.1016/j.actbio.2009.01.007. Epub 2009 Jan 21. PMID: 19208503.

[13] Sjöström T, McNamara LE, Meek RM, Dalby MJ, Su B. 2D and 3D nanopatterning of titanium for enhancing osteoinduction of stem cells at implant surfaces. *Adv Healthc Mater.* 2013 Sep;2(9):1285-93. doi: 10.1002/adhm.201200353. Epub 2013 Mar 12. PMID: 23495107.

[14] Zhang W, Li Z, Liu Y, Ye D, Li J, Xu L, Wei B, Zhang X, Liu X, Jiang X. Biofunctionalization of a titanium surface with a nano-sawtooth structure regulates the behavior of rat bone marrow mesenchymal stem cells. *Int J Nanomedicine.* 2012;7:4459-72. doi: 10.2147/IJN.S33575. Epub 2012 Aug 13. PMID: 22927760; PMCID: PMC3422101.

[15] Zhengwei Li, Tianming Du, Changshun Ruan, Xufeng Niu, Bioinspired mineralized collagen scaffolds for bone tissue engineering, *Bioactive Materials*, Volume 6, Issue 5, 2021, Pages 1491-1511, ISSN 2452-199X, <https://doi.org/10.1016/j.bioactmat.2020.11.004>.

[16] Niu, Y.; Du, T.; Liu, Y. Biomechanical Characteristics and Analysis Approaches of Bone and Bone Substitute Materials. *J. Funct. Biomater.* 2023, 14, 212. <https://doi.org/10.3390/jfb14040212>.